Supporting Information

Coordination Polymer Gels with Modular Nano-morphologies, Tunable Emissions and Stimuli-responsive Behaviour Based on an Amphiphilic Tripodal Gelator

Papri Sutar and Tapas Kumar Maji*

Molecular Materials Laboratory, Chemistry and Physics of Materials Unit, Jawaharlal Nehru Centre for Advanced Scientific Research, Jakkur, Bangalore 560 064, India, Email: tmaji@jncasr.ac.in

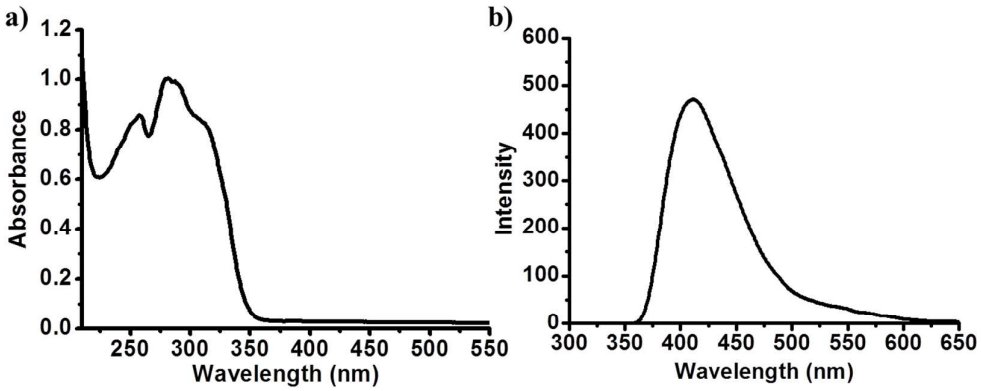

Figure S1. a) Absorption spectrum of **L** (10^{-4} M) in methanol, b) Emission spectrum of **L** (10^{-4} M) in methanol.

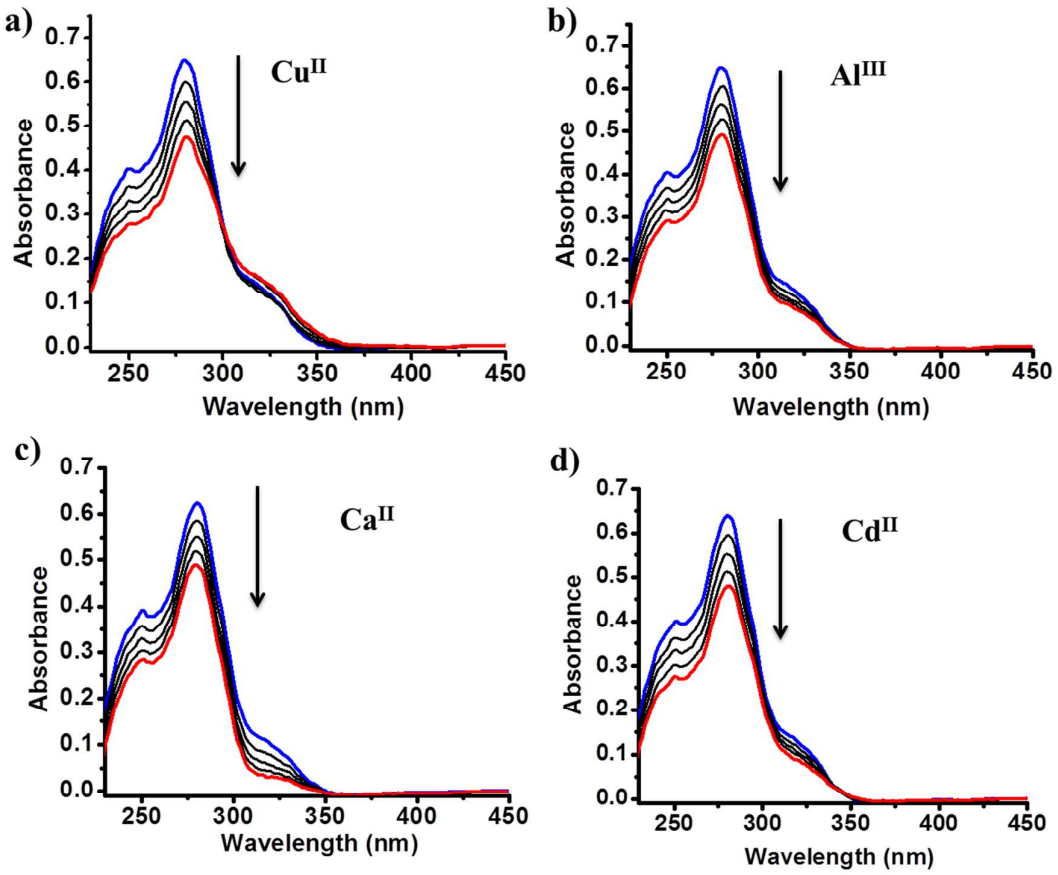

Figure S2. a), b), c), d) Change in absorption spectra of methanolic solution of **L** (10^{-5} M) after addition of methanolic solution of $Cu(NO_3)_2 \cdot 4H_2O$ (10^{-4} M), $Al(NO_3)_3$(10^{-4} M), $CaCl_2 \cdot 2H_2O$ (10^{-4} M) and $Cd(NO_3)_2$ (10^{-4} M) respectively. The blue curve is the absorption spectrum of **L** (1.5 ml, 10^{-5} M) and the red curve is the absorption spectrum of **L** after addition of 400µl (10^{-4} M) metal solution. The arrow indicates decrease in absorption intensity which is probably happening due to dilution effect.

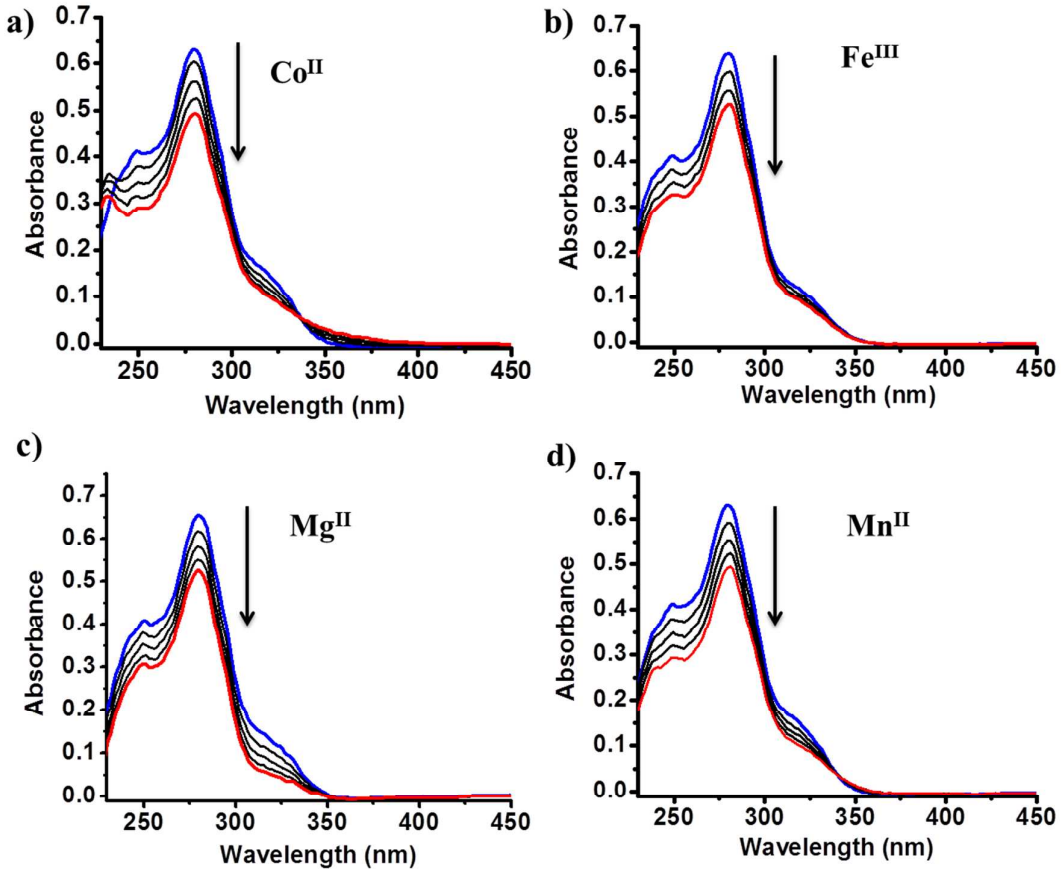

Figure S3. a), b), c), d) Change in absorption spectra of methanolic solution of **L** (10^{-5} M) after addition of methanolic solution of $Co(NO_3)_2 \cdot 6H_2O$ (10^{-4} M), $Fe(ClO_4)_3 \cdot H_2O$(10^{-4} M), $Mg(NO_3)_2 \cdot 6H_2O$ (10^{-4} M) and $Mn(NO_3)_2 \cdot 4H_2O$ (10^{-4} M) respectively. The blue curve is the absorption spectrum of **L** (1.5 ml, 10^{-5} M) and the red curve is the absorption spectrum of **L** after addition of 400µl (10^{-4} M) metal solution. The arrow indicates decrease in absorption intensity which is probably happening due to dilution effect.

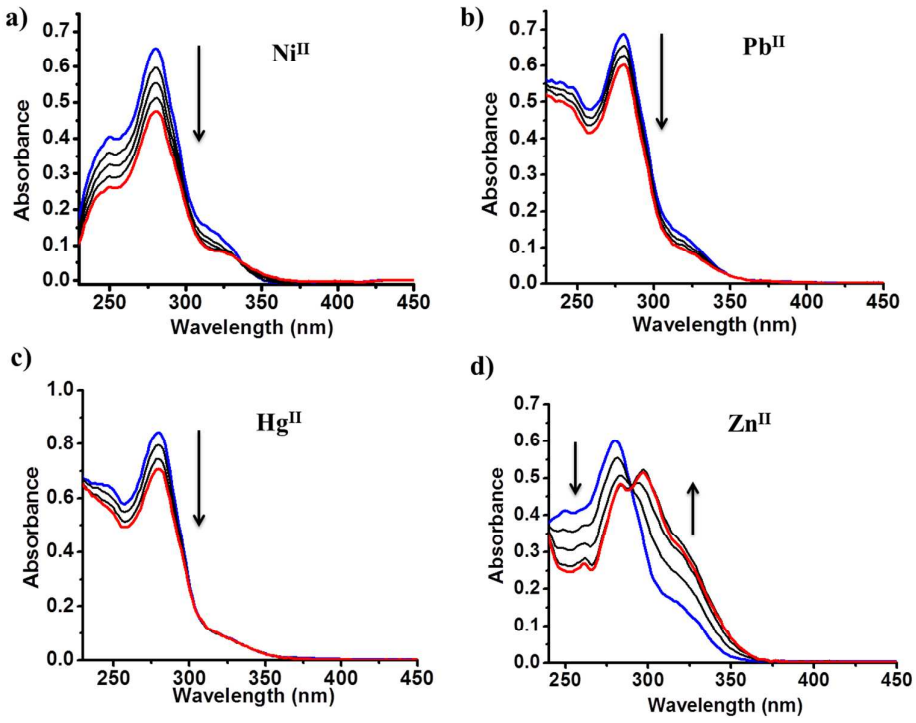

Figure S4. a), b), c), d) Change in absorption spectra of methanolic solution of **L** (10^{-5} M) after addition of methanolic solution of $Ni(NO_3)_2 \cdot 6H_2O$ (10^{-4} M), $Pb(NO_3)_2$(10^{-4} M), $HgCl_2$ (10^{-4} M) and $Zn(NO_3)_2 \cdot 6H_2O$ (10^{-4} M) respectively. The blue curve is the absorption spectrum of **L** (1.5 ml, 10^{-5} M) and the red curve is the absorption spectrum of **L** after addition of 400µl (10^{-4} M) metal solution. In a), b), c) the arrow indicates decrease in absorption intensity which is probably happening due to the dilution effect. In d) the arrows indicate change in absorption spectrum of **L** due to coordination of Zn^{II}.

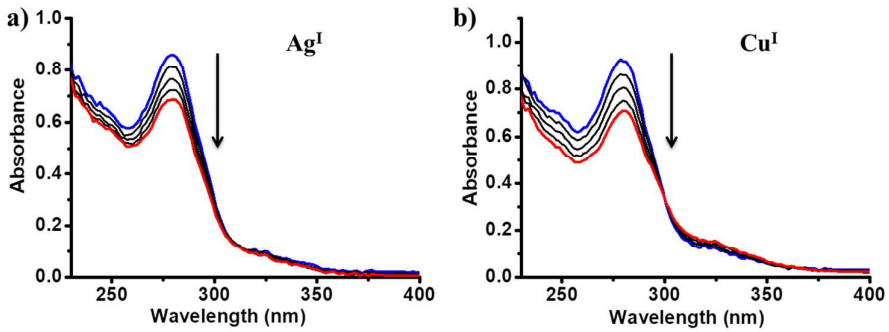

Figure S5. a), b) Change in absorption spectra of methanolic solution of **L** (10^{-5} M) after addition of methanolic solution of $AgNO_3$ (10^{-4} M) and CuI (10^{-4} M in 1:1 H_2O/MeOH) respectively. The blue curve is the absorption spectrum of **L** (1.5 ml, 10^{-5} M) and the red curve is the absorption spectrum of **L** after addition of 400µl (10^{-4} M) metal solution. The arrow indicates decrease in absorption intensity which is probably happening due to dilution effect.

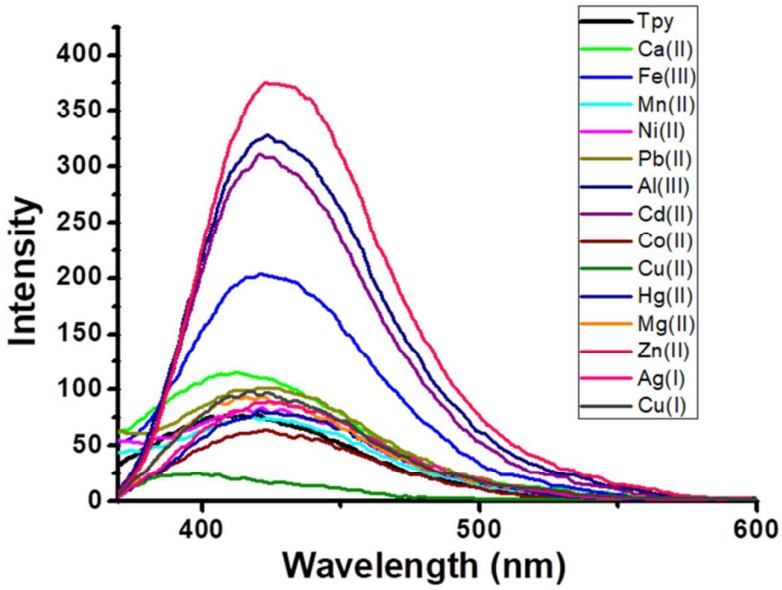

Figure S6. Change in emission spectra of methanolic solution of 2,2':6',2''-terpyridin-4-yl-propane-1,3-diamine (10^{-5} M) after addition of methanolic solution of different metal ions. The final concentration of metal ions in the mixture is 1.5×10^{-5} M in all cases.

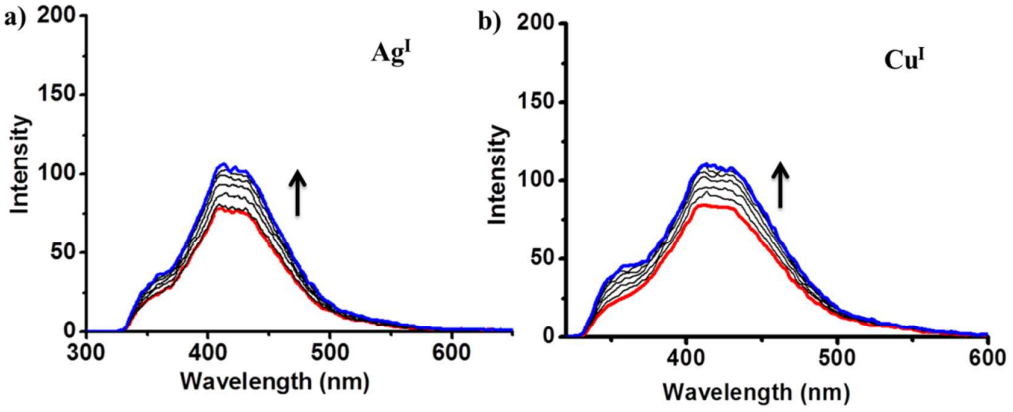

Figure S7. Change in emission spectra of methanolic solution of **L** (10^{-5} M) after addition of methanolic solution of a) $AgNO_3$ and b) CuI (in 1:1 MeOH/H_2O mixture)

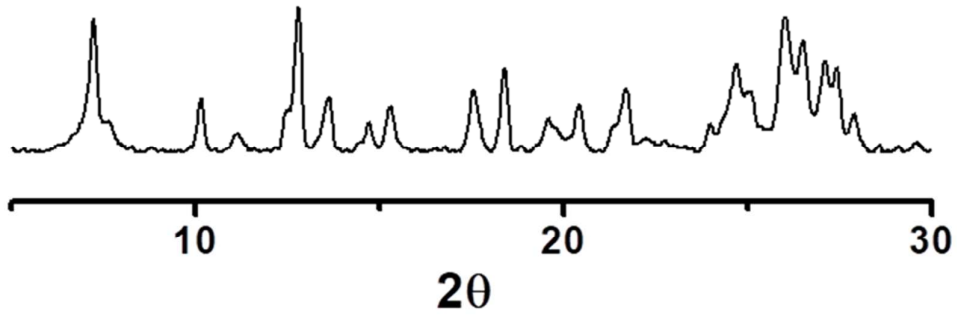

Figure S8. PXRD pattern of the precipitate obtained after addition of 1.5 equivalents of Zn^{II} during the formation of **ZnL** gel.

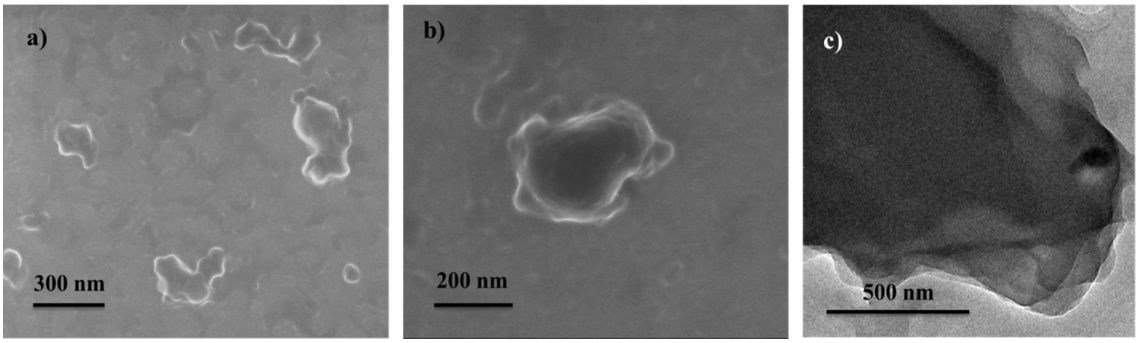

Figure S9. a), b) FESEM images of **ZnL** xerogel showing formation of irregular sheets, c) TEM images of **ZnL** xerogel showing the presence of layered sheets.

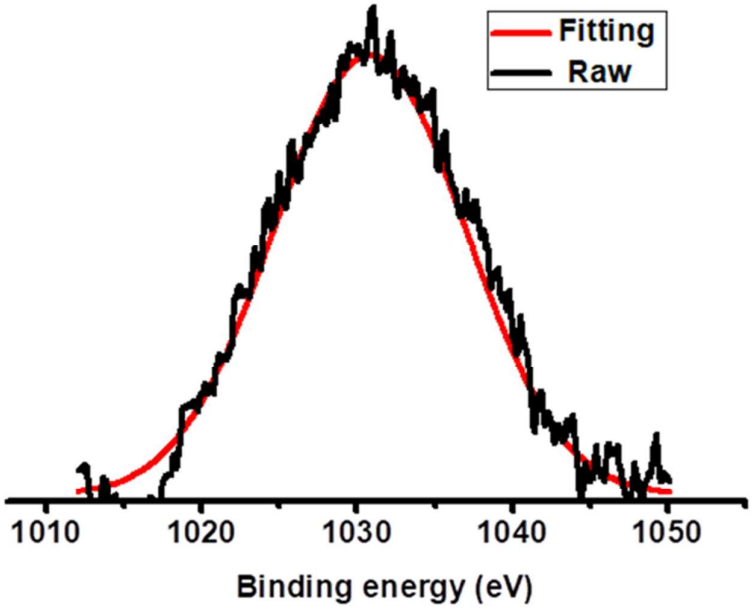

Figure S10. The XPS transition of Zn 2p in **ZnL**.

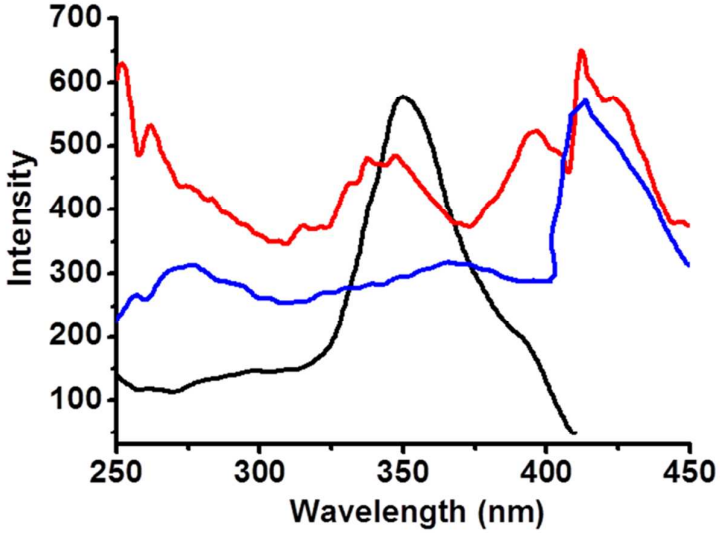

Figure S11. Excitation spectra of **L** (10^{-4} M, in methanol, black), **HG** xerogel (blue) and **ZnL** xerogel (red).

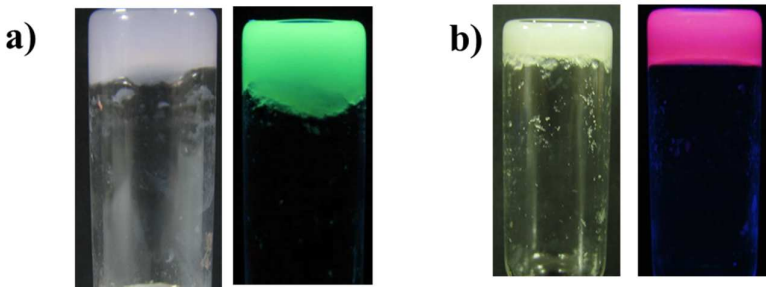

Figure S12. a) Photograph of **TbL** gel under day light (left) and UV-light (right), b) Photograph of **EuL** under day light (left) and UV-light (right).

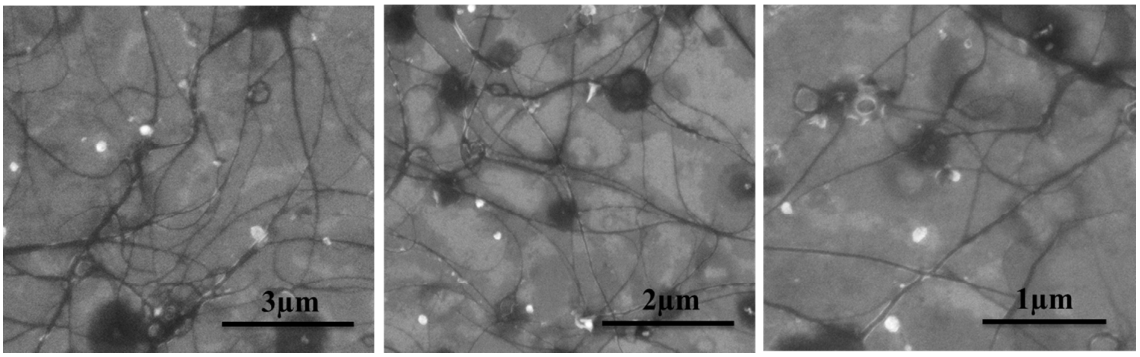

Figure S13. FESEM images of **TbL** xerogel.

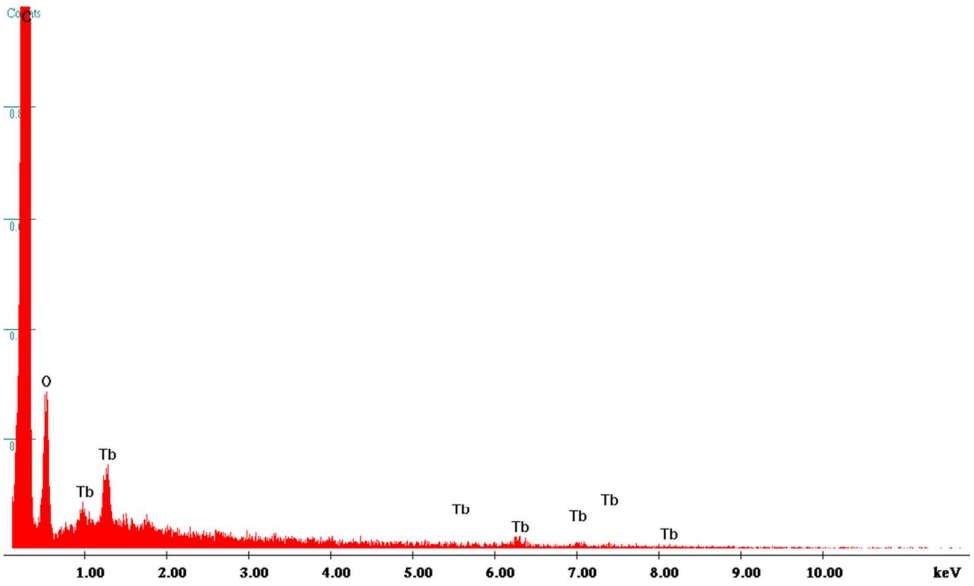

Figure S14. EDAX of **TbL** showing the presence of Tb^{III}.

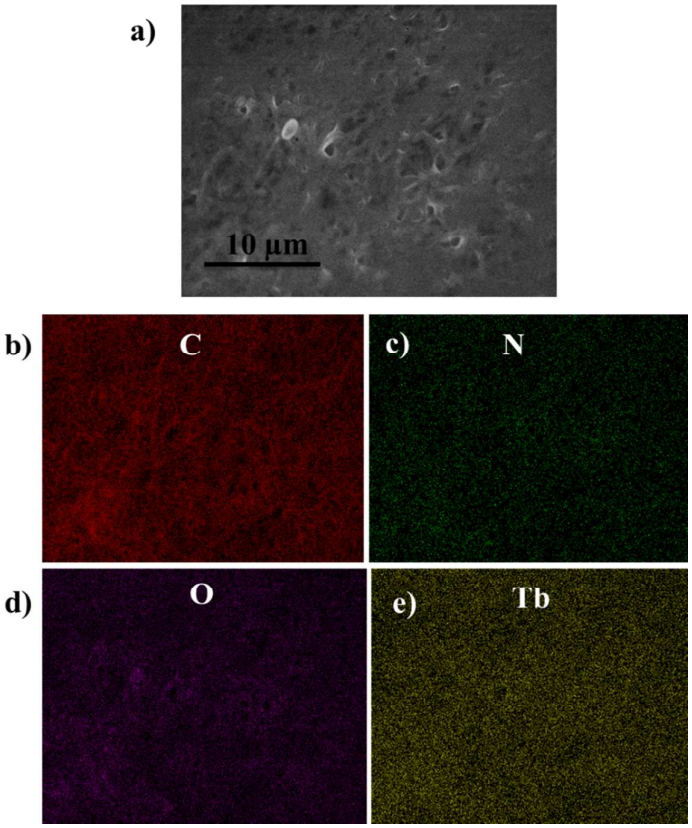

Figure S15. a) FESEM image of the **TbL** xerogel network where elemental mapping was performed. Elemental mapping of b) C, c) N, d) O and e) Tb^{III} showing uniform distribution of all the elements.

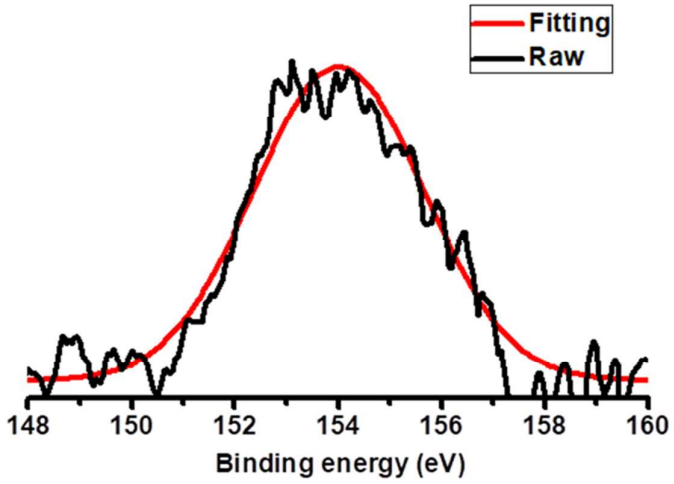

Figure S16. The XPS transition of Tb 4d in **TbL**.

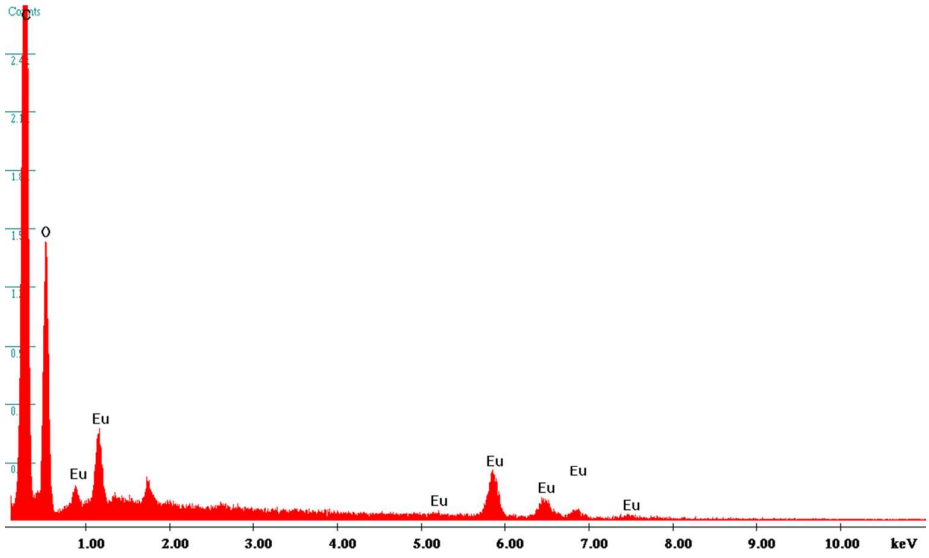

Figure S17. EDAX of **EuL** showing the presence of Eu^{III}.

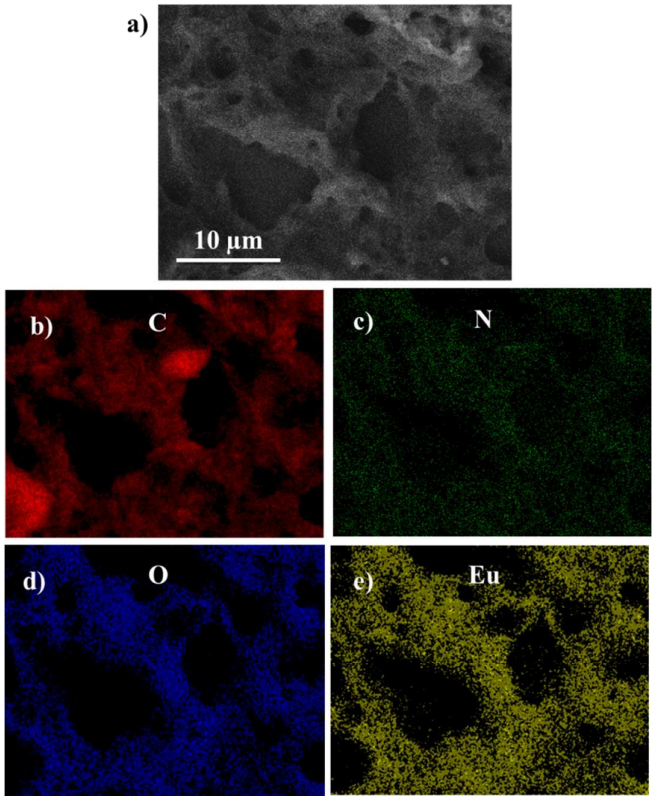

Figure S18. a) FESEM image of the **EuL** xerogel network where elemental mapping was performed. Elemental mapping of b) C, c) N, d) O and e) Eu^{III} showing uniform distribution of all the elements.

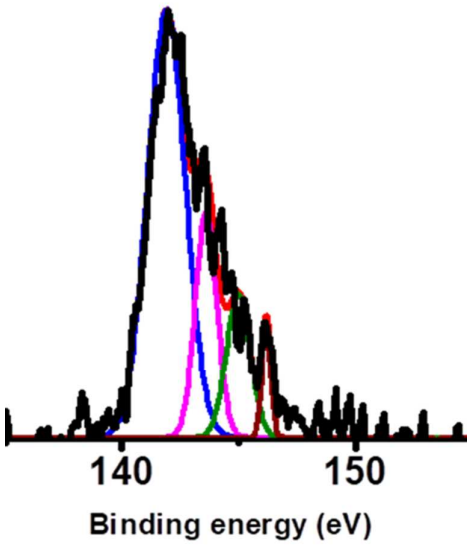

Figure S19. XPS transition of Eu 4d in **EuL.**

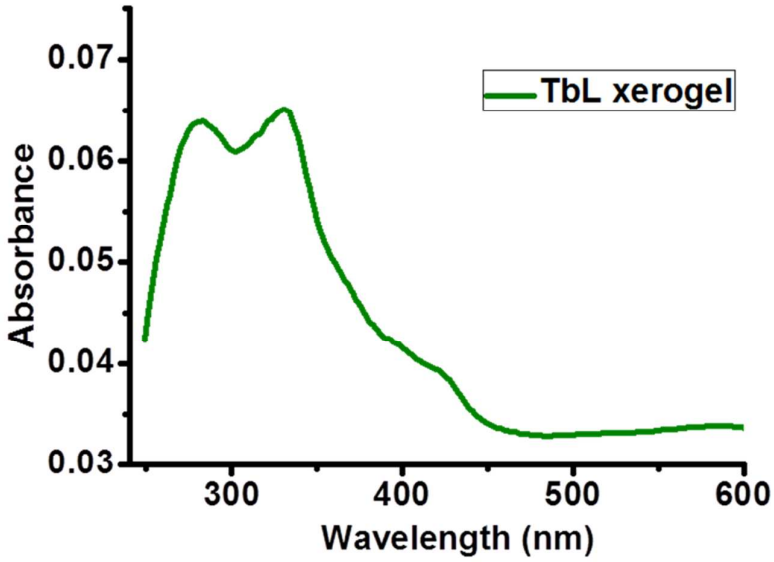

Figure S20. Absorption spectrum of **TbL** xerogel.

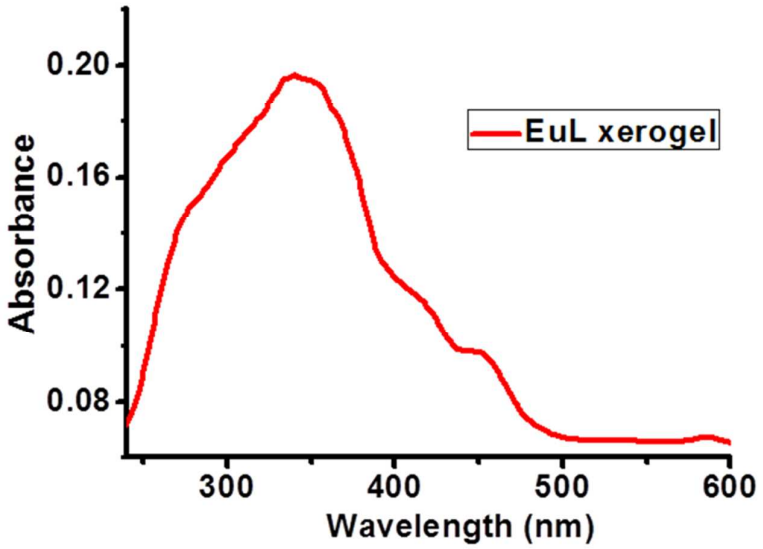

Figure S21. Absorption spectrum of **EuL** xerogel.

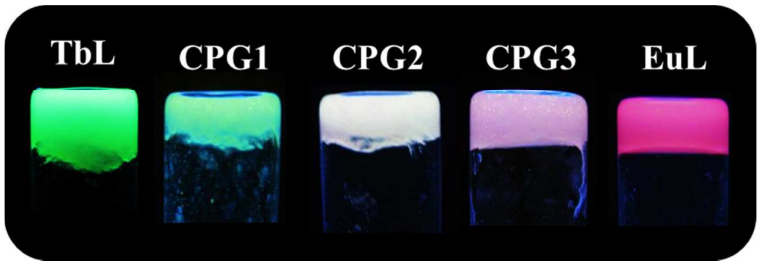

Figure S22. Photograph of **TbL**, **CPG1**, **CPG2**, **CPG3**, **EuL** gels under UV light showing green, cyan, white, pink and red emission respectively.

Compound	τ	QY
TbL	**303 µs (at 543 nm)**	**5.3%**
EuL	**1 ms (at 616 nm)**	**18.4%**
CPG1	**205 µs (at 543 nm)**	**7.6%**
CPG2	**165 µs (at 543 nm)**	**21.7%**
CPG3	**150 µs (at543 nm)**	**7.6%**

Table S1: The lifetime and quantum yield values of **TbL**, **EuL**, **CPG1**, **CPG2** and **CPG3**.

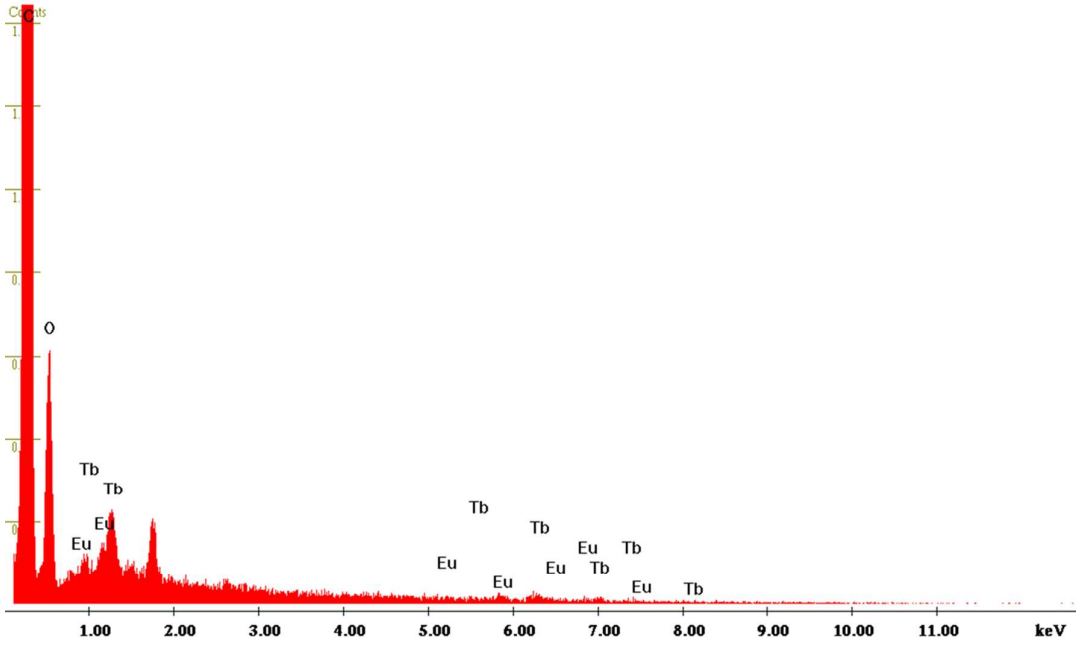

Figure S23. EDAX of **CPG1** showing the presence of both Tb^{III} and Eu^{III}.

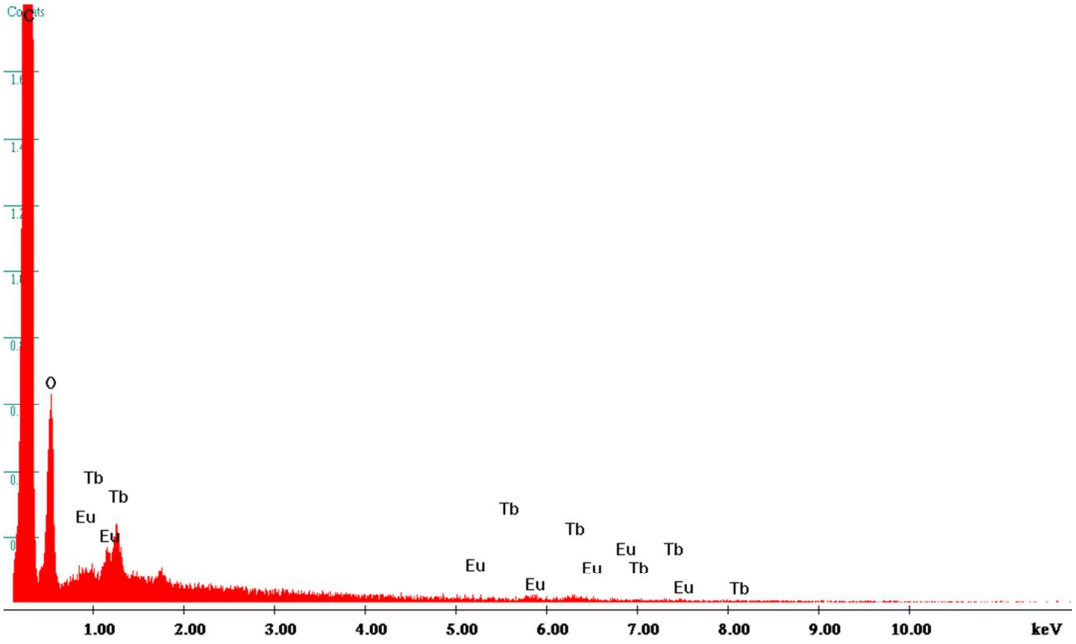

Figure S24. EDAX of **CPG2** showing the presence of both Tb^{III} and Eu^{III}.

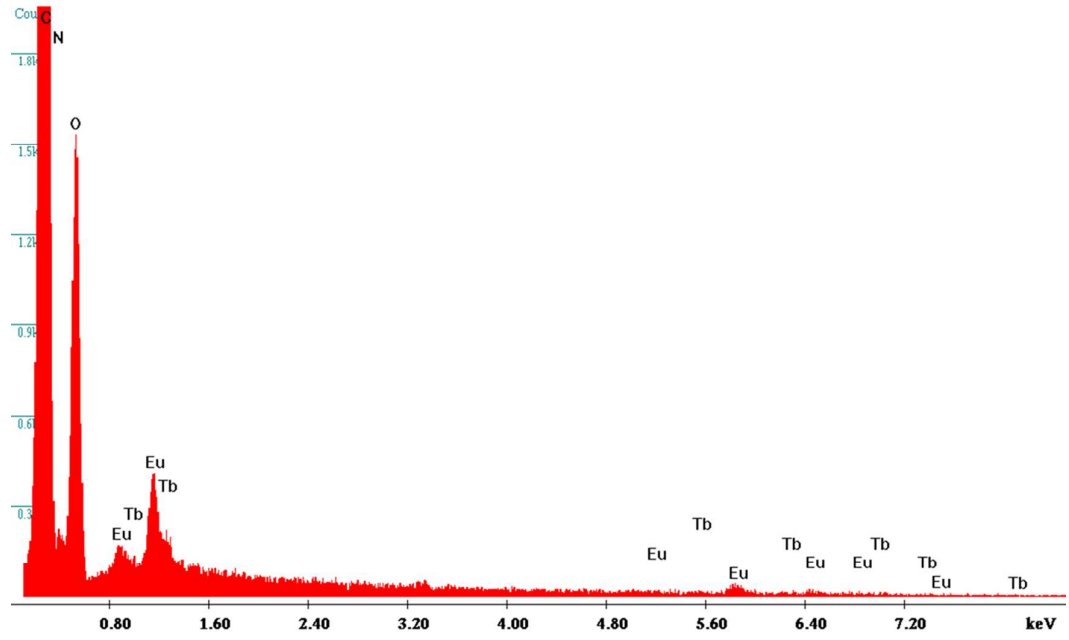

Figure S25. EDAX of **CPG3** showing the presence of both Tb^{III} and Eu^{III}.

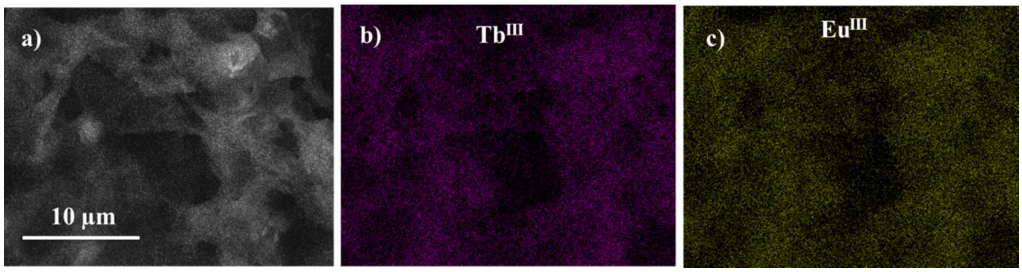

Figure S26. a) FESEM image of the **CPG2** xerogel network where elemental mapping was performed. Elemental mapping of b) Tb^{III} and c) Eu^{III} showing uniform distribution of both the metal ions throughout the **CPG2** network.

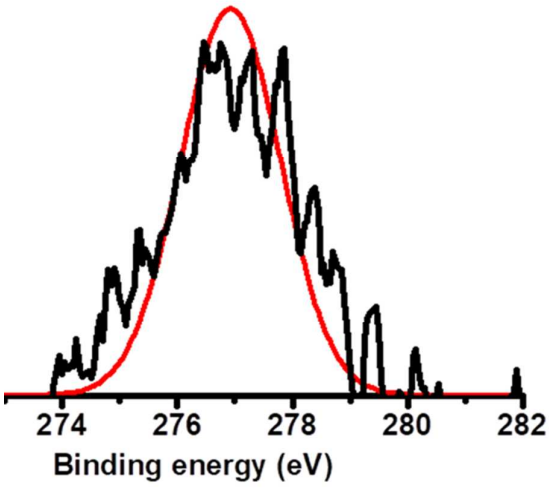

Figure S27. The XPS transition of Tb 4d in **CPG2.**

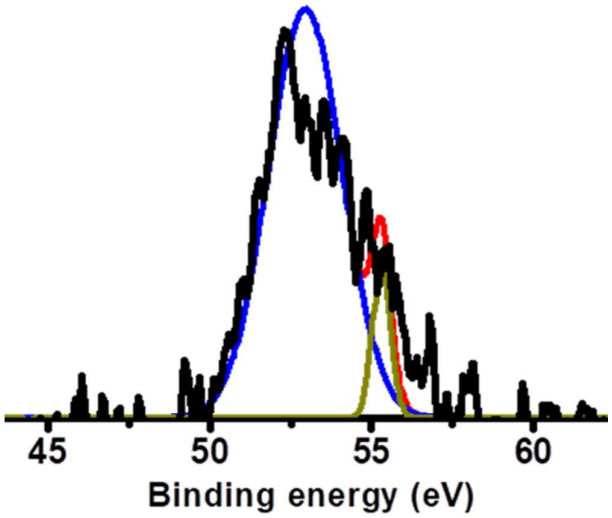

Figure S28. The XPS transition of Eu 5s in **CPG2.**

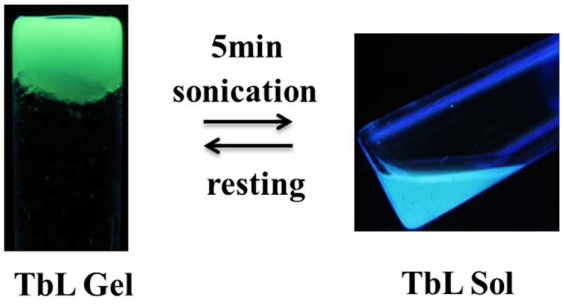

Figure S29. Sonication induced reversible gel to sol transition of **TbL**. The **TbL** gel showing green emission and **TbL** sol is showing blue emission under UV light.

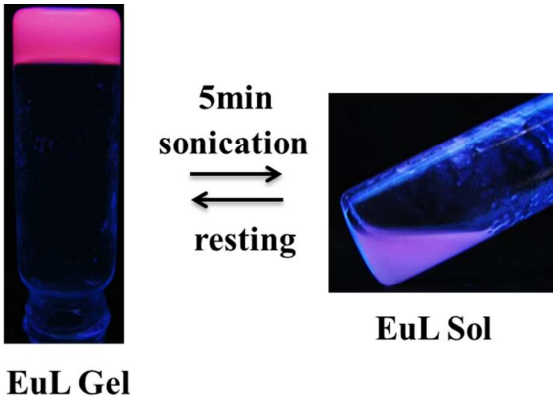

Figure S30. Sonication induced reversible gel to sol transition of **EuL**. The **EuL** gel showing red emission and **EuL** sol is showing bluish pink emission under UV light.

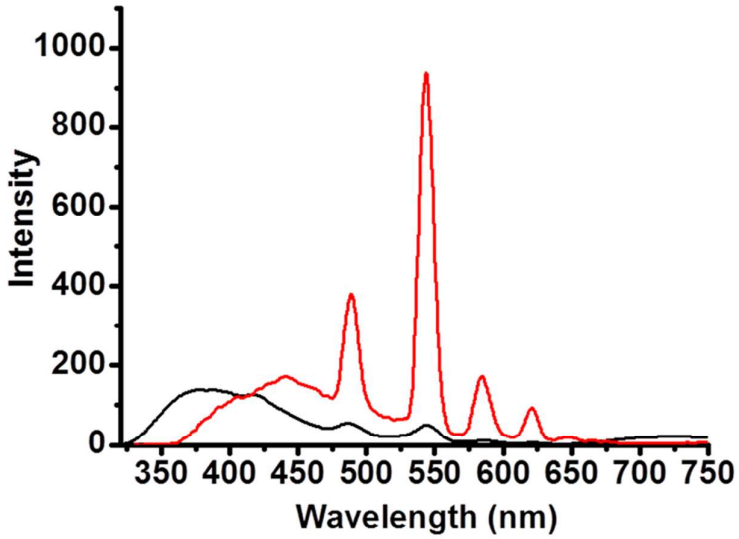

Figure S31. Emission spectra of **TbL** gel (red) and **TbL** sol (black).

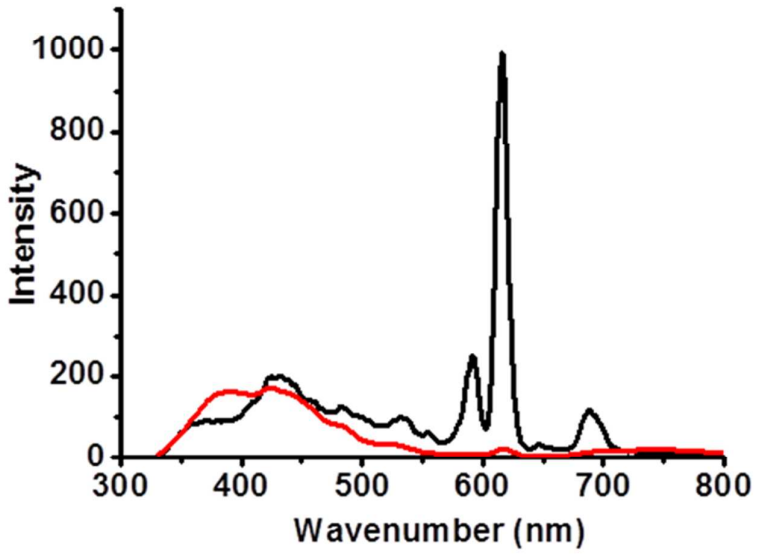

Figure S32. Emission spectra of **EuL** gel (red) and **EuL** sol (black).

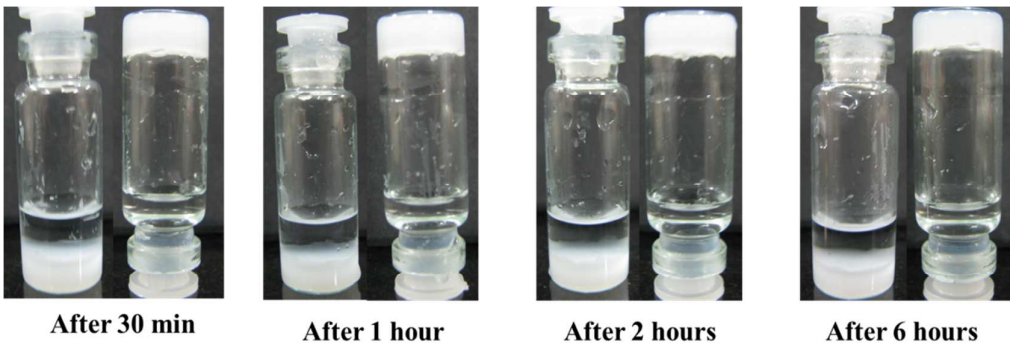

Figure S33. Pictures of **TbL** gel with 1 ml water layered on the top. No gel to sol transition was observed after 6 hours.